

## Cationic Oligonucleotide–Peptide Conjugates with Aggregating Properties Enter Efficiently into Cells while Maintaining Hybridization Properties and Enzymatic Recognition

Andrew W. Fraley,<sup>†</sup> Bénédicte Pons, Deniz Dalkara, Gérard Nullans, Jean-Paul Behr, and Guy Zuber\*

Contribution from the Université Louis Pasteur de Strasbourg, Laboratoire de Chimie Génétique associé au CNRS, Faculté de Pharmacie, BP 60024, 67401 Illkirch, France

Received February 12, 2006; E-mail: zuber@bioorga.u-strasbg.fr

**Abstract:** Oligonucleotide delivery is a crucial issue for therapeutical purposes and is often addressed by conjugation to short cationic peptides although with controversial results. To further examine this mechanism, a 15-mer anionic oligonucleotide was conjugated to a cationic peptide in order to obtain a diblock compound with an overall positive charge with aggregation properties. These microaggregates were efficiently internalized in cells via the expeditious pathway used by commercial gene delivery systems. Moreover, stability of the duplex formed with the complementary sequence increased without inhibiting oligonucleotide enzyme recognition as shown by the properties of the conjugate to prime chain elongation by Taq DNA polymerase in a linear amplification/sequencing process.

### Introduction

Commercially available gene delivery molecules are based on polycationic molecules or micelles that interact electrostatically and quasi-irreversibly with the anionic nucleic acids to form aggregates with an overall cationic surface charge.<sup>1–3</sup> These micrometric aggregates in turn anchor to the external face of cell plasma membranes by electrostatic interactions with proteoglycans<sup>4</sup> and are engulfed into intracellular compartments (endosomes and lysosomes) dedicated to content degradation. At this stage, the quantity of internalized complexes per vacuole and subversion of some enzyme-based cellular mechanism such as vacuole acidification using proton-sponge polymers<sup>5,6</sup> or chloroquine<sup>7</sup> may lead to the rupture of the vacuolar membranes, gene escape into the cytosol, and eventually gene translocation into the nucleus and (gene) expression. Remarkably, much larger quantities of material are internalized in adherent cell lines via cationic aggregation<sup>8</sup> than other more receptor-specific path-

ways;<sup>9,10</sup> furthermore, some cationic vectors initially designed for gene delivery were shown to be also efficient for protein<sup>11,12</sup> and oligonucleotide translocation.<sup>13</sup> However, shortening the nucleic acid segment approximately 100-fold weakens electrostatic cohesion of these complexes, which can then no longer withstand competition with larger polyanions present in biological fluids or cell surfaces.<sup>14</sup> One solution for exploiting this efficient pathway is to covalently link the oligonucleotide to a cationic chain that is longer than the oligonucleotide. Electrostatic zipping of the covalently linked tails with the anionic oligonucleotide may induce aggregation of the neutralized domains (or condensation) and direct the excess cationic segments toward the surface of the precipitates. In addition, cationization of an oligonucleotide should favorably impact hybridization by reducing interstrand electrostatic repulsion (e.g., PNA,<sup>15,16</sup> aegPNA,<sup>17</sup> phosphorodiamidate morpholino-oligonucleotides,<sup>18</sup> ODN with cationic bases,<sup>19</sup> or cationic ODN<sup>20,21</sup>). Finally, keeping the natural phosphodiester backbone may

<sup>†</sup> Current address: Ensemble Discovery Corp., 99 Erie St, Cambridge, MA 02139.

- (1) Demeneix, B.; Hassani, Z.; Behr, J. P. *Curr. Gene Ther.* **2004**, *4*, 445–55.
- (2) Zhang, S.; Xu, Y.; Wang, B.; Qiao, W.; Liu, D.; Li, Z. *J. Controlled Release* **2004**, *100*, 165–80.
- (3) Merlin, J. L.; Dolivet, G.; Dubessy, C.; Festor, E.; Parache, R. M.; Verneuil, L.; Erbacher, P.; Behr, J. P.; Guillemin, F. *Cancer Gene Ther.* **2001**, *8*, 203–10.
- (4) Mislack, K. A.; Baldeschwieler, J. D. *Proc. Natl. Acad. Sci. U.S.A.* **1996**, *93*, 12349–54.
- (5) Boussif, O.; Lezoualch, F.; Zanta, M. A.; Mergny, M. D.; Scherman, D.; Demeneix, B.; Behr, J. P. *Proc. Natl. Acad. Sci. U.S.A.* **1995**, *92*, 7297–7301.
- (6) Kichler, A.; Leborgne, C.; Coeytaux, E.; Danos, O. *J. Gene Med.* **2001**, *3*, 135–44.
- (7) Erbacher, P.; Roche, A. C.; Monsigny, M.; Midoux, P. *Exp. Cell Res.* **1996**, *225*, 186–94.
- (8) Labat-Moleur, F.; Steffan, A. M.; Brisson, C.; Perron, H.; Feugeas, O.; Furstenberger, P.; Oberling, F.; Brambilla, E.; Behr, J. P. *Gene Ther.* **1996**, *3*, 1010–1017.

- (9) Vives, E. *J. Controlled Release* **2005**, *109*, 77–85.
- (10) Zuber, G.; Zammuto-Italiano, L.; Dauty, E.; Behr, J. P. *Angew. Chem., Int. Ed.* **2003**, *42*, 2666–9.
- (11) Zelphati, O.; Wang, Y.; Kitada, S.; Reed, J. C.; Felgner, P. L.; Corbeil, J. *J. Biol. Chem.* **2001**, *276*, 35103–10.
- (12) Dalkara, D.; Zuber, G.; Behr, J. P. *Mol. Ther.* **2004**, *9*, 964–9.
- (13) Spagnou, S.; Miller, A. D.; Keller, M. *Biochemistry* **2004**, *43*, 13348–56.
- (14) Chittimalla, C.; Zammuto-Italiano, L.; Zuber, G.; Behr, J. P. *J. Am. Chem. Soc.* **2005**, *127*, 11436–41.
- (15) Nielsen, P. E. *Mol. Biotechnol.* **2004**, *26*, 233–48.
- (16) Nielsen, P. E. *Methods Mol. Biol.* **2005**, *288*, 343–58.
- (17) D'Costa, M.; Kumar, V. A.; Ganesh, K. N. *J. Org. Chem.* **2003**, *68*, 4439–45.
- (18) Nelson, M. H.; Stein, D. A.; Kroeker, A. D.; Hatlevig, S. A.; Iversen, P. L.; Moulton, H. M. *Bioconjugate Chem.* **2005**, *16*, 959–66.
- (19) Potier, P.; Abdennaji, A.; Behr, J. P. *Chemistry* **2000**, *6*, 4188–94.
- (20) Szabo, I. E.; Bruce, T. C. *Bioorg. Med. Chem.* **2004**, *12*, 4233–44.
- (21) Michel, T.; Martinand-Mari, C.; Debart, F.; Lebleu, B.; Robbins, I.; Vasseur, J. J. *Nucleic Acids Res.* **2003**, *31*, 5282–90.

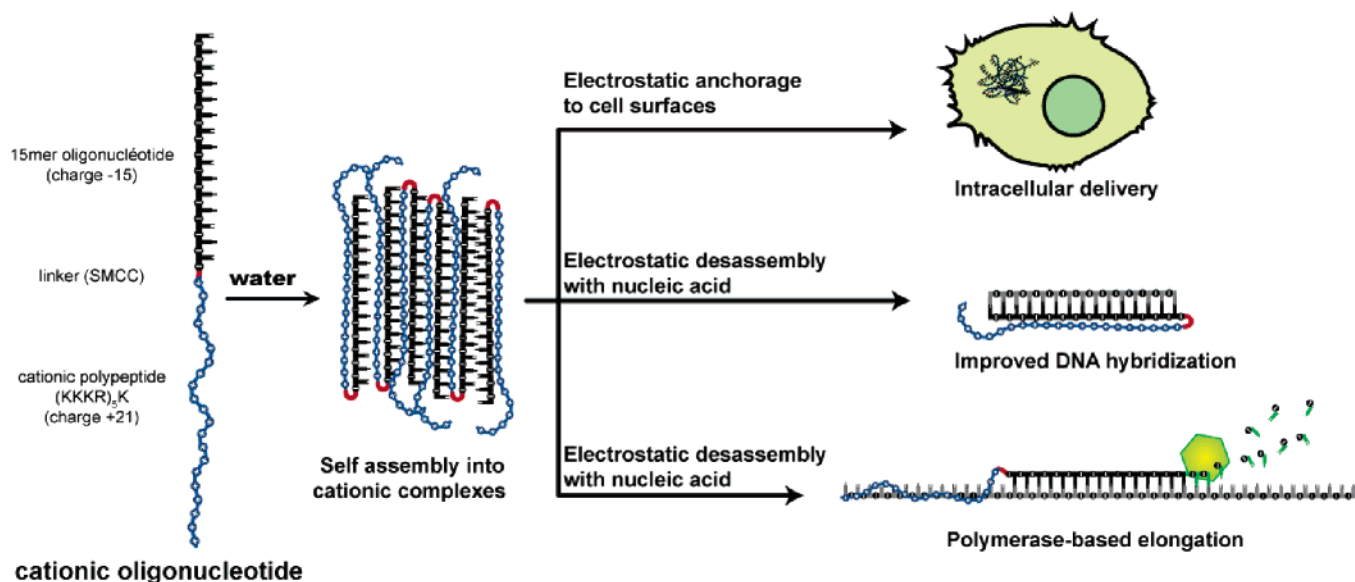


**Figure 1.** Schematic representation of the cationic diblock oligonucleotide and its properties.

preserve enzyme binding properties and their beneficial consequences.<sup>22</sup> Not unexpectedly, conjugation of oppositely charged polymers raises multiple synthetic challenges<sup>23,24</sup> and to date has only led to the synthesis and study of natural oligodeoxynucleotide conjugates that exhibit a net negative charge.<sup>25–27</sup> We have developed a method for conjugating a natural 15 nt long oligodeoxyribonucleotide to trifluoroacetyl-protected cationic peptides at its 5' end resulting in molecules with net negative (−5), neutral, and positive (+6) charge after aminolysis. The cationic oligonucleotide showed interesting biophysical and biological properties (Figure 1).

## Materials and Methods

**Materials.**  $\alpha$ -NH<sub>2</sub>-Fmoc protected amino acids, preloaded resin, and reagents were purchased from Novabiochem, Merck KgaA (Darmstadt, Germany). All oligonucleotides were purchased from Eurogentec (Seraing, Belgium). All other chemicals were purchased from Sigma-Aldrich (St. Louis, MO) unless otherwise noted. UV/vis analysis was performed on a Uvonik spectrometer, and  $T_m$  data for ODN duplexes were obtained on a Cary100 UV/vis spectrometer. HPLC purifications were performed on HP 1100 HPLC systems using the following methods: Method A, gradient of 2.5%–70% acetonitrile with 0.1% TFA was run over 40 min at 3 mL/min using a semipreparative Vydac C-4 column with detection at 220 nm; Method B, a gradient of 2.5%–70% acetonitrile with 50 mM triethylammonium acetate (TEAA, pH 7.0) was run over 40 min at 1.5 mL/min using a 4.6 mm  $\times$  250 mm Agilent C-18 column with detection at 260 nm; Method C, a gradient of 30%–70% acetonitrile with 1 M TEAA solution (pH 7.0) was run over 40 min at 2 mL/min using a semipreparative Vydac C-4 column with detection at 260 nm. Mass spectral ionizations (MS) were obtained using electrospray (ES), matrix-assisted laser desorption/ionization (MALDI) techniques that were coupled with time-of-flight (TOF) detectors, and conjugate mass spectral data were acquired using a Waters quadrupole time-of-flight (QTOF) mass spectrometer in negative mode. Each peptide was diluted in MeOH/H<sub>2</sub>O/HCOOH (50/50/0.5)

at 1  $\mu$ M concentration for ES analysis. Alpha-cyano-4-hydroxycinnamic acid was used as the matrix for the MALDI analysis.

**Peptide Synthesis.** Peptides were prepared using standard automated solid-phase Fmoc chemistry on Wang resin preloaded with  $\beta$ -alanine using *O*-(benzotriazol-1-yl)-*N,N,N',N'*-tetramethyluronium hexafluorophosphate (HBTU) as a condensing agent. For hand coupling, a portion of dried peptide grafted resin (300 mg, 0.31 mmol/g) was swelled for 1 h in dry DMF (1 mL) to which was added hydroxybenzotriazole (HOBt, 63.7 mg), PyBOP (237 mg), and  $N\alpha$ -Fmoc-S-trityl-cysteine (272 mg) in a spin chromatography column. The sealed column was shook for 1 h, the resin was washed with fresh DMF, and the coupling was repeated. After completion of the reaction, the resin was washed with DMF (5 mL), EtOH (5 mL), and CH<sub>2</sub>Cl<sub>2</sub> (5 mL) and then dried and stored until needed. The dried resin was swollen in dichloromethane for 1 h, filtered to remove excess solvent, and placed in a round-bottom flask. Cleavage from the support and removal of acid labile protecting groups were afforded by overnight treatment with 10 mL of a 95% trifluoroacetic acid/2.5% water/2.5% triisopropylsilane (TIS) solution. The resin was removed via filtration, and the resulting filtrate was concentrated to  $\sim$ 2 mL by rotary evaporation and placed on ice. Cold diethyl ether (15 mL) was added to facilitate precipitation of the crude peptide. The crude peptide was dissolved in 50%/50% acetonitrile/H<sub>2</sub>O (0.1% TFA) solution and purified by HPLC (Method A). The isolated product was lyophilized to dryness and then dissolved in 5 mL of 1/1 CH<sub>3</sub>CN/H<sub>2</sub>O solution. Purified peptide concentration was determined using the TBNS assay for free terminal primary amine, and additionally for free sulfide via Ellman's assay.<sup>28</sup>

**Peptide Characterization.** **CK(tfa)[R[K(tfa)]<sub>3</sub>]<sub>5</sub>- $\beta$ Ala:** HPLC retention time (Method A): 22.68 min. MALDI-TOF-MS ( $m/z$ ): calcd for C<sub>164</sub>H<sub>248</sub>F<sub>48</sub>N<sub>54</sub>O<sub>40</sub>S (M), 4557.7986; found, 4562.22 (MH<sup>+</sup>). ES-MS ( $m/z$ ): 913.7422 ((MH<sub>5</sub>/5)<sup>+</sup>, 100%), 1140.4496 ((MH<sub>4</sub>/4)<sup>+</sup>, 70%). **C-[K(tfa)]<sub>3</sub>-[R[K(tfa)]<sub>3</sub>]<sub>3</sub>- $\beta$ Ala:** HPLC retention time (Method A): 22.50 min. ES-MS ( $m/z$ ): calcd for C<sub>120</sub>H<sub>180</sub>F<sub>36</sub>N<sub>38</sub>O<sub>30</sub>S (M), 3349.2873; found, 1117.4596 (MH<sub>3</sub>/3, 100%)<sup>+</sup>. **C-[K(tfa)]<sub>2</sub>-[R[K(tfa)]<sub>3</sub>]<sub>2</sub>- $\beta$ Ala:** HPLC retention time (Method A): 16.54 min. ES-MS ( $m/z$ ): calcd for C<sub>82</sub>H<sub>124</sub>F<sub>24</sub>N<sub>26</sub>O<sub>21</sub>S (M), 2296.8772; found, 1149.1056 (MH<sub>2</sub>/2)<sup>+</sup>, 1160.0717 ((MHN<sub>a</sub>/2)<sup>+</sup>, 80%).

**SMCC-Oligonucleotide Synthesis.** A lyophilized purified oligonucleotide 5'-NH<sub>2</sub> (CH<sub>2</sub>)<sub>6</sub>-p-CGAGGGCGAGGGCGA (1  $\mu$ mol synthesis) was dissolved in 20 mM sodium phosphate (pH 8.0) to provide a 1 OD/10  $\mu$ L solution. *N*-Succinimidyl 4-(maleimidomethyl)-cyclo-

(22) Ishihara, T.; Corey, D. R. *Nucleic Acids Symp. Ser.* **1999**, 141–2.  
 (23) Tung, C. H.; Stein, S. *Bioconjugate Chem.* **2000**, *11*, 605–18.  
 (24) Prater, C. E.; Miller, P. S. *Bioconjugate Chem.* **2004**, *15*, 498–507.  
 (25) Chen, C. P.; Zhang, L. R.; Peng, Y. F.; Wang, X. B.; Wang, S. Q.; Zhang, L. H. *Bioconjugate Chem.* **2003**, *14*, 532–8.  
 (26) Turner, J. J.; Arzumanov, A. A.; Gait, M. J. *Nucleic Acids Res.* **2005**, *33*, 27–42.  
 (27) Zatspein, T. S.; Turner, J. J.; Oretskaya, T. S.; Gait, M. J. *Curr. Pharm. Des.* **2005**, *11*, 3639–54.

(28) Riddles, P. W.; Blakeley, R. L.; Zerner, B. *Anal. Biochem.* **1979**, *94*, 75–81.

hexanecarboxylate (40 equiv, 45 mM) in DMF was added to the oligonucleotide, and the reaction was allowed to shake at ambient temperature for 1 h, after which a second 40 equiv amount in DMF of activated SMCC was added to the reaction mixture. The mixture was allowed to sit at ambient temperature overnight, and for reactions where the oligonucleotide tethered a fluorescein label, the reaction was kept in the dark. Upon completion of incubation, the reaction mixture was concentrated under reduced pressure to approximately 100  $\mu$ L and purified by size exclusion chromatography using an NAP-10 desalting column (Amersham Biosciences, Uppsala Sweden). HPLC (Method B) confirmed product formation. The same protocol was used for the fluorescein labeled oligonucleotide starting with a 5'-NH<sub>2</sub>-(CH<sub>2</sub>)<sub>6</sub>-p-CGAGGGCGAGGGCGA-p-fluorescein oligonucleotide (1  $\mu$ mol synthesis) except that the reaction was performed in the dark. HPLC retention times (Method B): 12.15 min (5'-H<sub>2</sub>N-CGAGGGCGAGGGCGA), 16.25 min (5'-maleimide-CGAGGGCGAGGGCGA), 15.05 min (5'-H<sub>2</sub>N-CGAGGGCGAGGGCGA-3'-fluorescein), 17.60 min (5'-maleimide-p-CGAGGGCGAGGGCGA-3'-fluorescein).

**Synthesis of tfa-Protected Conjugates.** For a typical reaction, freshly diluted SMCC-oligonucleotide (8 nmol) in 10  $\mu$ L of 1 M HEPES buffered with triethylamine (pH 7.0), 10  $\mu$ L of 1 M tris-[carboxyethyl]-phosphine, and 80  $\mu$ L of DMF were added to the corresponding peptide (40 nmol) dried via speed-vac in an eppendorf tube. The reaction mixture was well vortexed and allowed to sit at ambient temperature for 48 h, after which it was dried under reduced pressure. The resulting crude product was dissolved in 30% acetonitrile/1 M TEAA (pH 7.0). Isolation was afforded via reversed phase HPLC (method C). The purified conjugate was lyophilized to dryness for long-term storage. For further handling, the conjugates (obtained in 10 to 20% yield) were dissolved in 80% DMF/H<sub>2</sub>O (0.1 mL).

**Conjugate Characterization.** 5'-maleimide-p-CGAGGGCGAGGGCGA: HPLC retention time (Method C): 6.5 min. 5'-maleimide-p-CGAGGGCGAGGGCGA-p-fluorescein: HPLC retention time (Method C): 8.0 min. ( $\beta$ -Ala[[K(tfa)]<sub>3</sub>R]<sub>5</sub>K(tfa)Cys-p-CGAGGGCGAGGGCGA: HPLC retention time (Method C): 11.7 min. QTOF-MS (*m/z*): calcd for C<sub>330</sub>H<sub>460</sub>F<sub>48</sub>N<sub>125</sub>O<sub>131</sub>P<sub>15</sub>S (M), 9677.8194; found, 1379.3875 ([M - 7H]/7), 1206.8534 ([M - 8H]/8), 1072.7814 ([M - 9H]/9).  $\beta$ -Ala[[K(tfa)]<sub>3</sub>R]<sub>5</sub>K(tfa)Cys-p-CGAGGGCGAGGGCGA-p-fluorescein: HPLC retention time (Method C): 12.5 min. QTOF-MS (*m/z*): calcd for C<sub>358</sub>H<sub>486</sub>F<sub>48</sub>N<sub>126</sub>O<sub>140</sub>P<sub>16</sub>S (M), 10228.9540; found, 1460.4382 ([M - 7H]/7), 1278.1171 ([M - 8H]/8), 1135.5603 ([M - 9H]/9).  $\beta$ -Ala[[K(tfa)]<sub>3</sub>R]<sub>5</sub>[K(tfa)]<sub>3</sub>Cys-p-CGAGGGCGAGGGCGA: HPLC retention time (Method C): 9.8 min. QTOF-MS (*m/z*): calcd for C<sub>285</sub>H<sub>388</sub>F<sub>36</sub>N<sub>109</sub>O<sub>121</sub>P<sub>15</sub>S (M), 8453.2769; found, 1206.8376 ([M - 7H]/7), 1055.7371 ([M - 8H]/8), 938.3151 ([M - 9H]/9).  $\beta$ -Ala[[K(tfa)]<sub>3</sub>R]<sub>5</sub>[K(tfa)]<sub>3</sub>Cys-p-CGAGGGCGAGGGCGA: HPLC retention time (Method C): 8.5 min. QTOF-MS (*m/z*): calcd for C<sub>247</sub>H<sub>332</sub>F<sub>24</sub>N<sub>97</sub>O<sub>112</sub>P<sub>15</sub>S (M), 7400.8667; found, 1056.2596 ([M - 7H]/7), 924.1556 ([M - 8H]/8), 821.3215 ([M - 9H]/9).

**Deprotection.** Deprotection was performed in a tightly sealed 1.5-mL tube by addition of 0.5 mL of 28% NH<sub>4</sub>OH<sub>(aq)</sub> to 1 nmol of either single-stranded conjugate or its duplex with a natural complementary 15-mer. The mixture was heated at 55 °C for 6 h and lyophilized to yield quantitative deprotection.

**Thermal Stability Studies.** *T<sub>m</sub>* measurements were carried out on a Varian Cary UV-vis spectrometer with heating from 4 °C to 95 °C at rate of 1 °C/min and data sampling once every minute. A stream of N<sub>2</sub> gas was maintained over the cells until the temperature reached above 20 °C. Duplexes were dissolved in 10 mM Tris HCl, pH 7.0 buffer containing 150 mM NaCl (1-mL volume).

**Electrophoresis Mobility Assay.** Detection of the unlabeled conjugate was by hybridization to a strictly complementary strand (5'-TCGCCCTGCCCTCG), which was purchased with a fluorescein label at its 5' end. The labeled oligonucleotide strand (100 pmol) was mixed with ~1.1 equiv of the corresponding complementary unlabeled oligonucleotide or tfa-protected conjugate. Deprotection was then

performed by addition of 0.5 mL of 28% NH<sub>4</sub>OH<sub>(aq)</sub> for 6 h at 55 °C. After lyophilisation of all samples, residues were suspended in a loading buffer (10  $\mu$ L), consisting of TAE pH 7.0 buffer and 10% glycerol, and loaded onto a nondenaturing 15% polyacrylamide gel. Electrophoresis was run overnight in TAE pH 7.0 at 4 °C (5 V/cm). Fluorescence detection was performed using a Typhoon 8600 Imager.

**Cell Internalization Studies.** Cell culture media and supplements were from Sigma-Aldrich except for fetal bovine serum (Eurobio). BHK (ATCC number CCL-10), HeLa (ATCC number CCL-2) cells were cultured in Dulbecco's modified Eagle's medium (DMEM) supplemented with 10% fetal bovine serum (FBS), L-glutamine, and antibiotics. Cell lines were grown according to ATCC guidelines and were seeded at about 60 000 cells/well in 24-well tissue culture plates 1 day before the experiments. Cells were maintained at 37 °C in a 5% CO<sub>2</sub> humidified air atmosphere. The labeled conjugates, the control oligonucleotides, or a mixture of oligonucleotide with 1 equiv of free peptide were added to HeLa or BHK cells at a final concentration of 200 nM in 1 mL of FBS-free cell culture medium. The cells were then incubated at 37 °C in a 5% CO<sub>2</sub> humidified air atmosphere for 4 h, after which the media were completed with serum (10%). In the experiments with chloroquine, the agent (80  $\mu$ M final concentration) was applied simultaneously with the oligonucleotide. Cells were observed by fluorescent microscopy at 4 and 8 h using a Zeiss Axiovert-25 inverted microscope equipped with epifluorescent illumination using appropriate filter sets. All images were taken consecutively using the same image acquisition parameters. The integrity of cellular plasma membrane was further checked using propidium iodide, a normally membrane-impermeable red fluorescent stain.

**Plasmid Sequencing.** The pEGFP-Luc plasmid was sequenced using an automatic ABI 3100 sequencer by polymerase (Taq) chain reaction using standard methodology. For each reaction, 5 pmol of primer and 500 ng of plasmid were used. Data were visualized using FinchTV software (version 1.3.1, Geospiza Inc).

## Results and Discussion

**Design of the Peptide–Oligonucleotide Conjugates.** To ensure sufficient sequence selectivity, an oligonucleotide, 15 units in length, was chosen and was functionalized at its 5'-terminus to carry a primary amine. The sequence 5'-CGAGGGCGAGGGCGA-3' corresponds to nucleotides 708–722 of the EGFP-Luc plasmid and is within the coding region of the enhanced green fluorescent protein (EGFP). We selected the well-known *N*-succinidimyl 4-(maleimidomethyl)-cyclohexanecarboxylate (SMCC) reagent as a cross-linker for its mild chemistry as well as for the stability of the thioether bond under physiological conditions and in the presence of reducing agents.<sup>29</sup> For the peptide moieties, we chose peptides containing native cationic amino acids to provide a tail with the highest possible charge density for optimal DNA binding and condensation.<sup>30</sup> We initially investigated arginine homopolymers with an N-terminal cysteine. The guanidinium group of arginine has a high p*K<sub>a</sub>* (12.5), thus ensuring full protonation over a broad pH range. Unfortunately, oligopeptides containing more than 6 arginines led to practically unrecoverable oligonucleotide precipitates upon mixing, even in the presence of a cationic exchange resin.<sup>25</sup> Although coupling may have occurred, neither analysis nor isolation of the reaction products could be performed. We thus redesigned the peptide moiety in order to mask most of the charge of the polypeptide during the conjugation reaction with a protecting group that is cleaved off

(29) Schelte, P.; Boeckler, C.; Frisch, B.; Schuber, F. *Bioconjugate Chem.* **2000**, *11*, 118–23.

(30) DeRouchey, J.; Netz, R. R.; Radler, J. O. *Eur. Phys. J. E.* **2005**, *16*, 17–28.

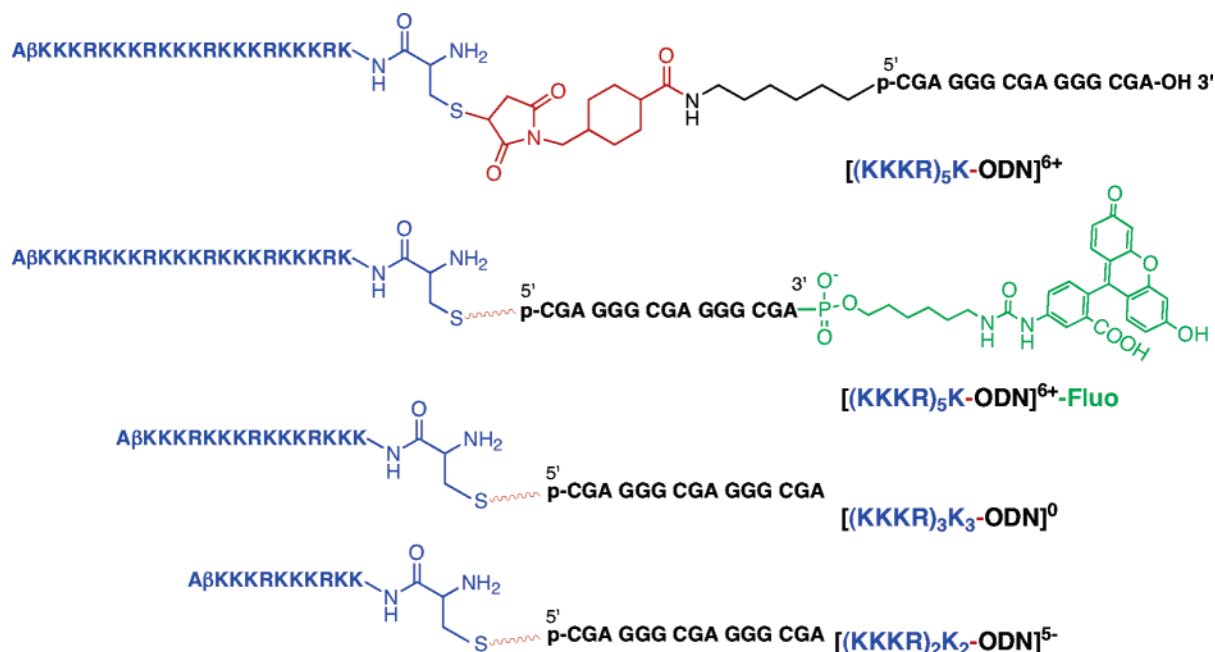


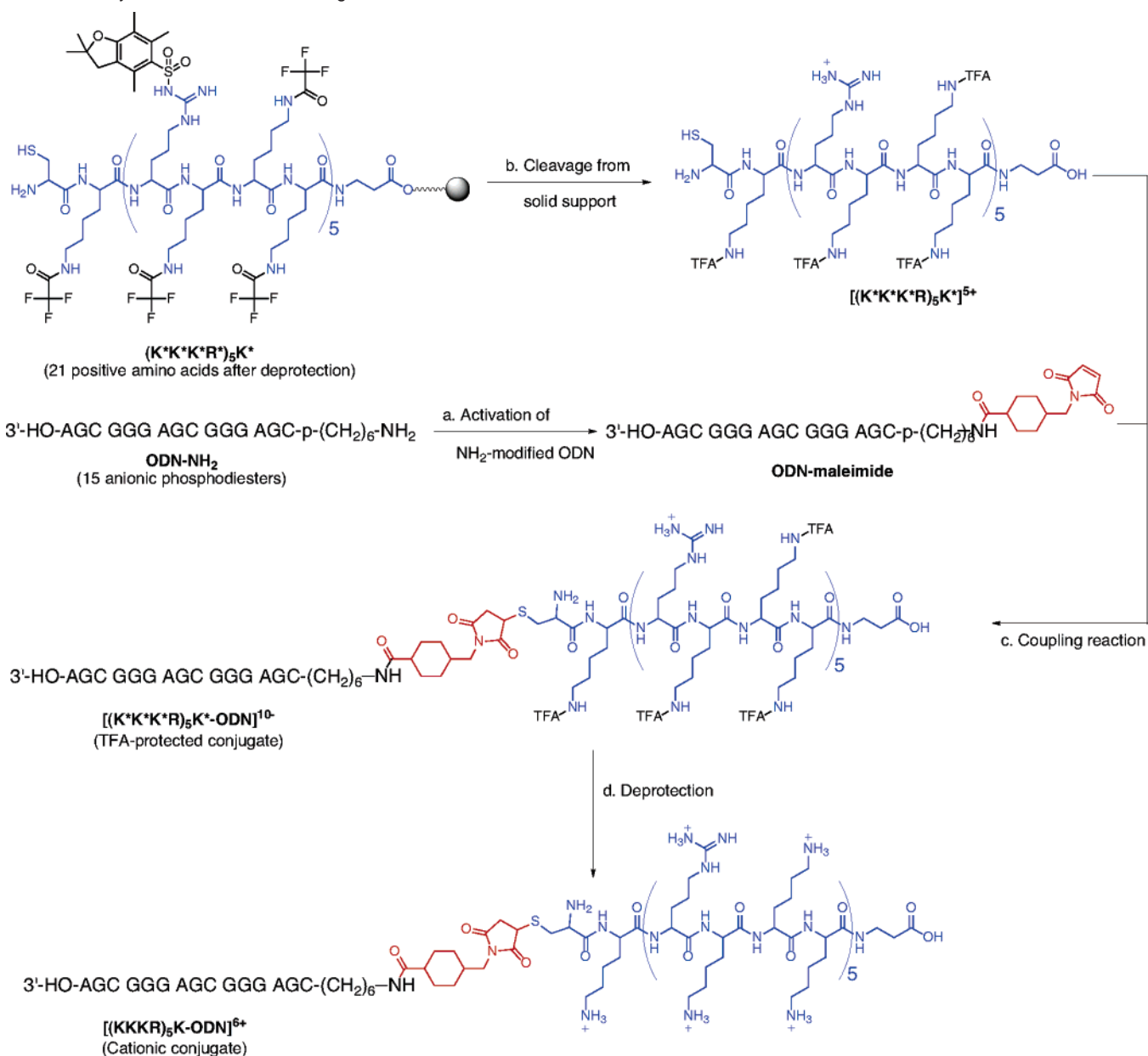
**Figure 2.** Chemical structure of the conjugates.

in conditions safe for oligonucleotides. Some arginines were replaced with *N* $\epsilon$ -trifluoroacetyl-protected lysines, as this protection is compatible with automatic peptide synthesis and is removable after conjugation by hydrolysis with aqueous ammonia. To counterbalance the poor solubility of the *N* $\epsilon$ -trifluoroacetyl-protected peptide, arginine residues were incorporated between several lysines using two sequence motifs (KKR and KKKR) that were repeated to provide peptides with various lengths. The KKKR motif provided higher peptide yields and solubilized more readily. We therefore only developed conjugation chemistry with the KKKR motif (Figure 2).

**Synthesis of the Protected Conjugates.** Peptides were prepared via standard automated solid-phase methodology starting from Wang resin preloaded with 9-fluorenylmethoxycarbonyl (FMoc)- $\beta$ -alanine (Scheme 1). After deprotection with piperidine, condensation of commercially available *N* $\alpha$ -Fmoc-*N* $\epsilon$ -(trifluoroacetyl)-lysine and *N* $\alpha$ -Fmoc-*N* $\omega$ -(pentamethylidihydrobenzofuran-5-sulfonyl)-arginine was performed with *O*-(benzotriazol-1-yl)-*N,N,N',N'*-tetramethyluronium hexafluorophosphate (HBTU). The last N-terminal cysteine residue was added manually using *N* $\alpha$ -Fmoc-*S*-trityl-cysteine and PyBOP as the condensing agent. The peptide was then cleaved from the resin by acidic treatment, and the crude material was purified by semipreparative HPLC under acidic conditions to avoid air-mediated oxidation of the thiol. In parallel, the oligonucleotide tethering a 5'-(CH<sub>2</sub>)<sub>6</sub>NH<sub>2</sub> linker was functionalized with *N*-succinimidyl 4-(maleimidomethyl)-cyclohexanecarboxylate (SMCC) (Scheme 1). Upon completion of the reaction (i.e., when HPLC analysis of the reaction indicated quantitative conversion to the SMCC-oligo conjugate), size exclusion chromatography yielded the purified product. The maleimide-functionalized oligonucleotide was then reacted with thiol-containing peptides in 80% DMF solution buffered with 100 mM HEPES-NEt<sub>3</sub> at pH 7.0. Analysis of the reaction and purification were accomplished by reversed phase HPLC on a semipreparative C-4 column using 30%–70% acetonitrile buffered with 1 M TEAA pH 7.0. As represented in Figure 3 for the (KKKR)<sub>3</sub> peptide, the starting oligonucleotide elutes at

6.3 min, while the trifluoroacetyl (tfa)-protected conjugate shifts to an elution time of 11.7 min; additionally, injection of the unactivated oligonucleotide mixed with the TFA-peptide did not modify the elution time of the oligonucleotide. The trifluoroacetyl groups were then removed by aminolysis at 55 °C for 6 h because these conditions provided quantitative deprotection of a model peptide containing 16 tfa groups (Supporting Information, Figures S1 and 2). After lyophilisation, a conjugate that was self-aggregated in water or in aqueous solutions with low to medium salt concentrations (e.g., 150 mM, the physiological salt concentration) was obtained.

For cellular trafficking studies, a fluorescein-tagged cationic conjugate was prepared from the corresponding 3'-fluorescein-labeled oligonucleotide. Finally, variation of the conjugate net charge was obtained by using peptides with different lengths (see Figure 2 for conjugate structures). Direct characterization of the diblock conjugates proved to be difficult. Trifluoroacetyl-protecting groups interfered with aqueous solubility of the conjugates as well as with their electrophoretic mobility. Indeed, these diblock oligomers appeared to dissolve only in DMF/H<sub>2</sub>O (8/2) and remained in the well upon electrophoresis on a polyacrylamide gel (data not shown). Removal of the protecting groups did not ease characterization as it led to a conjugate made of two oppositely charged oligomers, where electrostatic interactions favor self-assembly. These difficulties were overcome by hybridization of the tfa-protected ODN conjugates to a complementary oligonucleotide strand. Hybridization was followed by removal of the protecting groups (55 °C, 6 h) and analysis of the hybrid duplexes by native polyacrylamide gel electrophoresis (Figure 4). As shown in Figure 4A (lane 4), the duplex formed between the tfa-protected conjugate tfa<sub>16</sub>-(KKKR)<sub>5</sub>K-ODN and 5'-fluorescein-labeled complementary strand had a much lower electrophoretic mobility than that of the corresponding homoduplex (lane 2). Removal of the tfa-protecting groups after duplex formation by aminolysis (lane 5) led to almost total disappearance of the fluorescent signal, as a consequence of precipitation in the well and concomitant fluorescence signal quenching. Aggregation was due to conjuga-

**Scheme 1.** Synthesis of the Cationic Oligonucleotide

tion. Indeed, addition of an equimolar amount of unconjugated (KKKR)<sub>5</sub>K peptide to the DNA duplex produced no significant aggregation or electrophoretic retardation (see Supporting Information). Finally, similar electrophoretic and physicochemical behavior was observed with the parental 3'-fluorescein (KKKR)<sub>5</sub>K-ODN-fluo conjugate (Figure 4B).

**Cell Internalization Studies.** The oligonucleotide conjugates aggregated in the cell culture medium, which favored sedimentation onto adherent cells. A 200 nM fluorescein-labeled oligonucleotide, either (tfa)<sub>16</sub>(KKKR)<sub>5</sub>K-oligonucleotide or (KKKR)<sub>5</sub>K-oligonucleotide, was added onto HeLa cells and incubated for 4 h in serum-free cell culture medium containing chloroquine as an endosomal escape agent. After replacing the medium with FBS-supplemented fresh medium, imaging of the control experiment using the oligonucleotide (Figure 5A) showed no detectable fluorescence associated with cells or with the surface of the culture plate. Conversely, (tfa)<sub>16</sub>(KKKR)<sub>5</sub>K-oligonucleotide or (KKKR)<sub>5</sub>K-oligonucleotide aggregates were

clearly visible, yet with a striking difference in their attachment patterns. The protected and still anionic aggregates of (tfa)<sub>16</sub>(KKKR)<sub>5</sub>K-oligonucleotide appeared indeed distributed on the cells and supporting surface (Figure 5B) indicating that internalization efficiency does not rely only on aggregation. In contrast, the overall cationic aggregates were mainly localized in intracellular compartments that resemble the endosomal compartments and confirmed the hypothesis that aggregates bearing cationic surfaces are critical for interaction with cells and subsequent internalization.

Next we used longer incubation times to see whether the conjugate could escape degradative pathways and reach the cytoplasm. To limit the problems due to chloroquine cytotoxicity for long incubation times, we switched to the more robust BHK cell line (Figure 6). Simple mixing of the oligonucleotide with the cationic peptide did not induce aggregation; hence no cellular uptake was observed (Figure 6A). On the other hand, cells incubated with 200 nM labeled cationic conjugate showed a

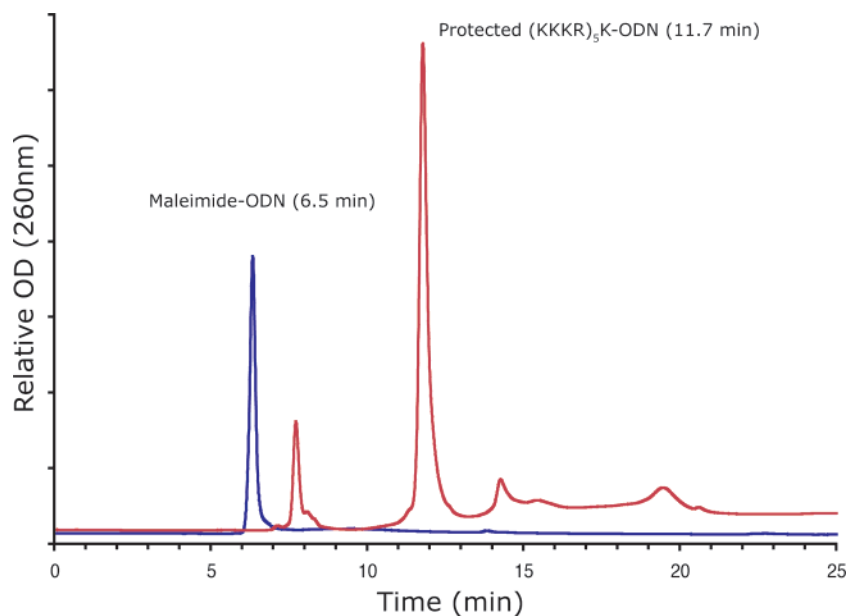


**Figure 3.** HPLC chromatographs of the maleimide-oligodeoxynucleotide (blue line) and of its reaction products with a 5-fold excess of thiolated and tfa-protected (KKKR)<sub>5</sub> peptide (red line). The product eluting at 11.7 min was assigned to the tfa-protected peptide–oligonucleotide conjugate.

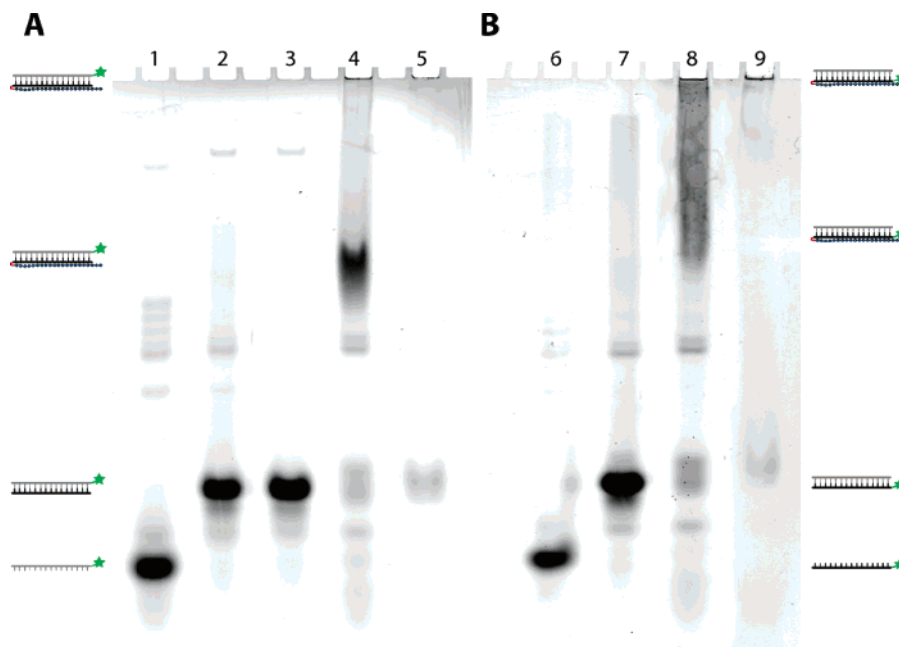


**Figure 4.** Analysis of the (KKKR)<sub>5</sub>K-ODN (A) and fluorescently labeled (KKKR)<sub>5</sub>K-ODN-fluo (B) by nondenaturing polyacrylamide gel electrophoresis via hybridization to a complementary oligonucleotide strand. Visualization of the unlabeled conjugate (gel A) and labeled conjugate (gel B) was by hybridization to a fluorescently tagged or untagged 5'-TCGCCCTCGCCCTCG probe, respectively. Lanes 1 and 6: fluorescently tagged single-strand probe. Lanes 2 and 7: duplexes with unmodified ODN. Lane 3: duplex subjected to aminolysis treatment. Lane 4: duplex with tfa-protected (KKKR)<sub>5</sub>K-ODN. Lane 5: (KKKR)<sub>5</sub>K-ODN duplex obtained by aminolysis of the corresponding protected duplex. Lane 8: duplex with tfa-protected (KKKR)<sub>5</sub>K-ODN-fluo. Lane 9: duplex with (KKKR)<sub>5</sub>K-ODN-fluo obtained by aminolysis of the corresponding tfa-protected duplex.

robust uptake after 8 h (Figure 6B, C), and in a number of cells, fluorescence had escaped from the vacuoles resulting in a diffuse pattern observed in the cytoplasm and the nucleus. The addition of 80  $\mu$ M chloroquine, which palliated the absence of buffering capacities of the peptide tail, increased the number of cells displaying diffuse intracellular fluorescence.

**Thermal Denaturation Studies.** Thermal denaturation profiles of duplexes formed by each conjugate and its complementary ODN strand were obtained in physiological salt concentrations (10 mM Tris·HCl, pH 7.0, 150 mM NaCl). Unfortunately, accurate determination of cationic oligonucleotide concentrations

was not possible, even in the presence of high concentrations of salt that weakened electrostatic interactions. Deprotecting the quantifiable TFA-protected conjugates in the presence of equimolar amounts of the complementary strand solved this problem. After lyophilisation, the duplex remained partially aggregated in water, but raising the salt concentration to 150 mM provided enough electrostatic shielding for solubilization of the oligonucleotides as estimated by UV titration at 260 nm. Measurement of melting temperatures of the different duplexes (Figure 7) resulted in an expected increase in thermal stability provided by charge neutralization of the phosphodiester back-

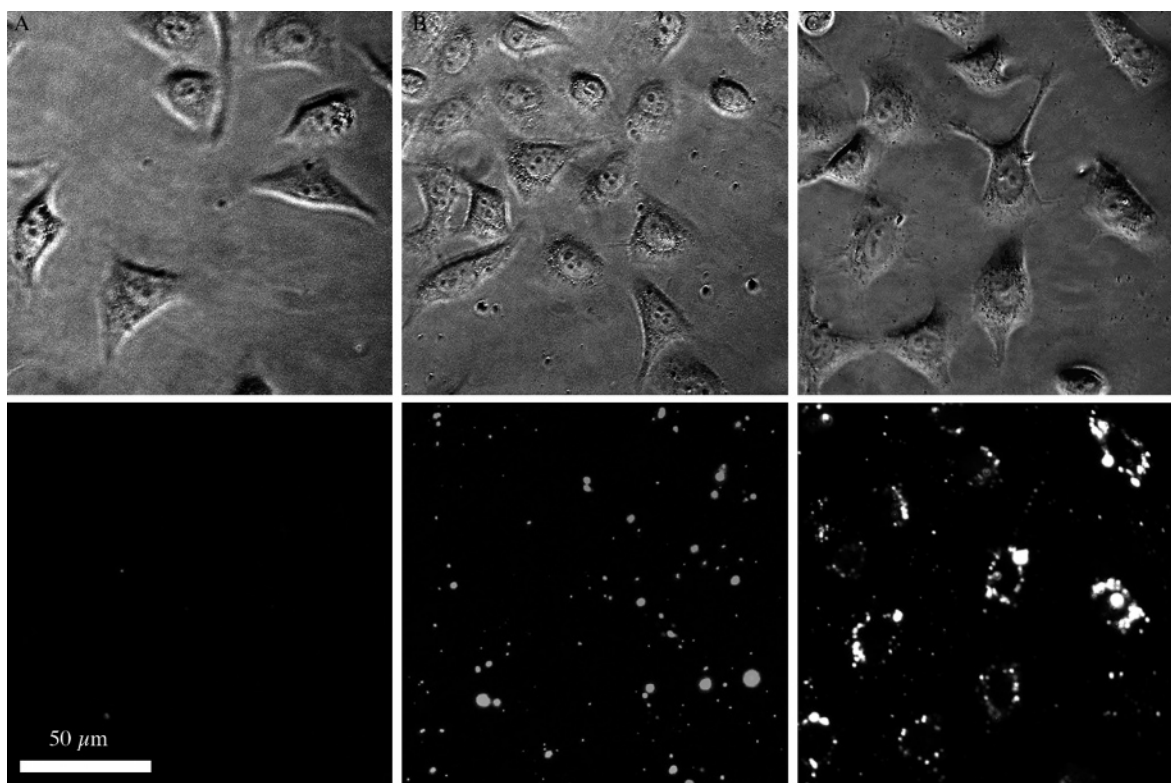


**Figure 5.** Cell internalization properties of (KKKR)<sub>5</sub>K-oligonucleotide aggregates. HeLa cells were incubated for 4 h in culture medium without serum in the presence of 80  $\mu$ M chloroquine and 200 nM fluorescein-labeled analogues of (A) oligonucleotide, (B) (tfa)<sub>16</sub>(KKKR)<sub>5</sub>K-oligonucleotide, or (C) cationic (KKKR)<sub>5</sub>K-oligonucleotide. Before visualization, the medium was removed and replaced with fresh medium containing 10% serum.

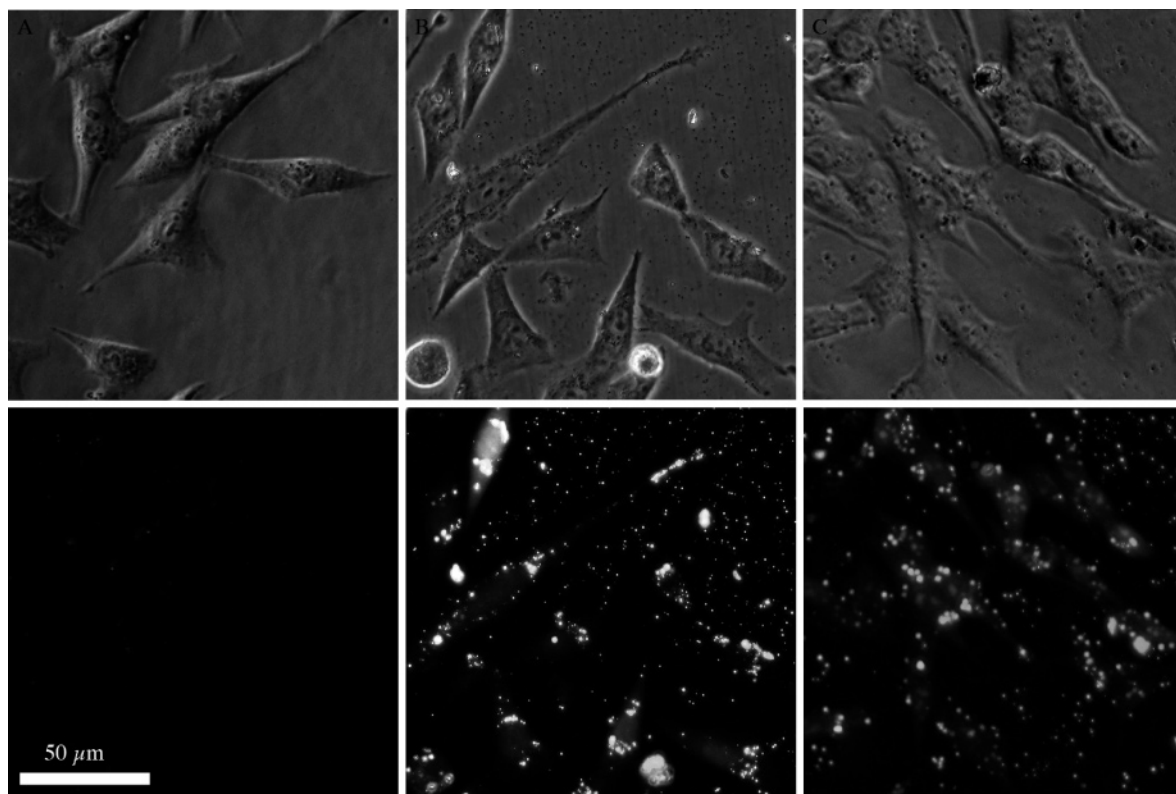


**Figure 6.** Cell internalization of fluorescein-labeled (KKKR)<sub>5</sub>K-oligonucleotide in BHK cells. Cells were incubated for 8 h in culture medium without serum in the presence of 200 nM (A) oligonucleotide and 200 nM unconjugated (KKKR)<sub>5</sub>K peptide, (B) (KKKR)<sub>5</sub>K-oligonucleotide, or (C) (KKKR)<sub>5</sub>K-oligonucleotide with 80  $\mu$ M chloroquine.

bone. A plot of  $T_m$  versus conjugate charge indicated a continuous increase in duplex stability, suggesting that longer

cationic tails may be even more potent. According to thermodynamics, the stability of the duplex should reach a plateau for

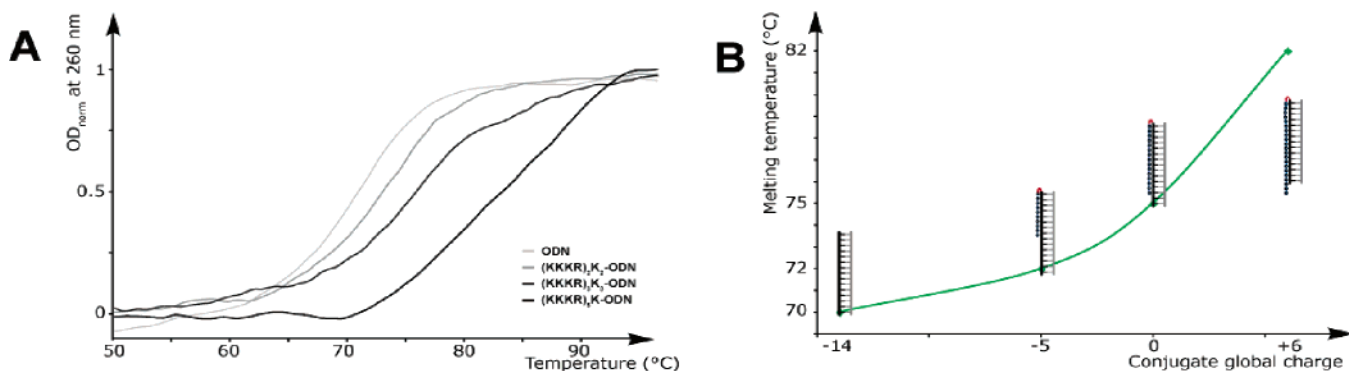


**Figure 7.** Effect of the cationic tail on duplexes' thermal stability. (A) Melting profiles of duplexes formed with (light gray) natural ODN<sup>-14</sup>, (medium gray) (KKKR)<sub>2</sub>K<sub>2</sub>-ODN<sup>-2</sup>, (dark gray) (KKKR)<sub>3</sub>K<sub>3</sub>-ODN<sup>0</sup>, and (black) (KKKR)<sub>5</sub>K<sub>5</sub>-ODN<sup>+6</sup> in 10 mM Tris HCl, pH 7.0 containing 150 mM NaCl. The Y-axis represents the normalized absorbance at 260 nm. (B) Histogram representing the variation of  $T_m$  versus conjugate global charge.

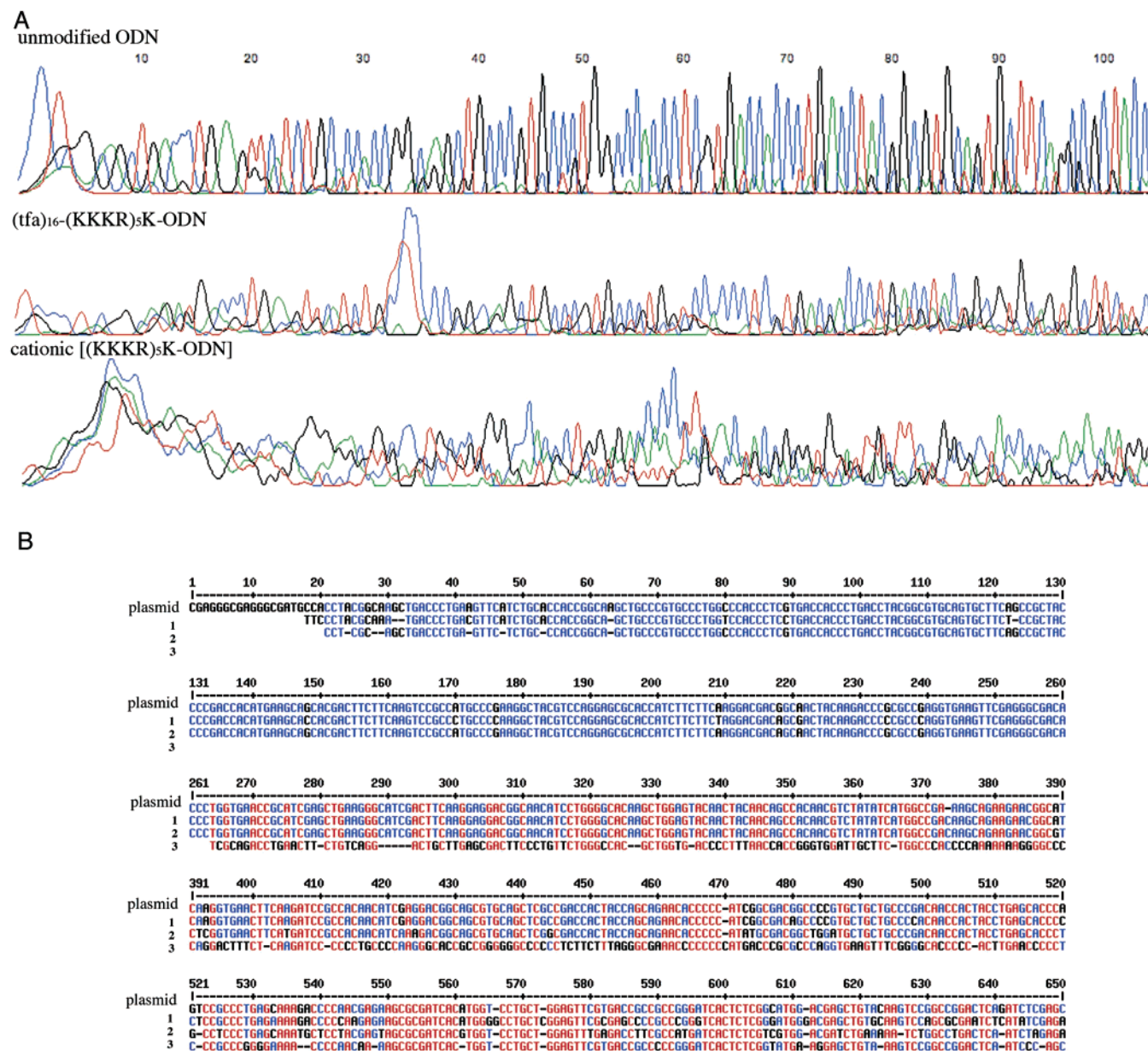


**Figure 8.** Automatic sequencing of the pEGFP-Luc plasmid using the natural or 5'-modified CGA GGG CGA GGG CGA oligonucleotides as primers for polymerase chain elongation. (A) Capillary electrophoresis traces of the end-fluorescent fragments corresponding to A (green), C (blue), G (black), and T (red). (B) Sequence alignment of the DNA fragments with plasmid elongated using the natural 15-mer oligonucleotide (1), the tfa-protected conjugate (2), and the cationic conjugate (3). Letters in red indicate a perfect match between all sequences.

charge neutralization. This means that the number of charges carried by the cationic tail could be up to twice that of the

oligonucleotide to provide optimal stability and eventually to strand invade the genomic duplex.<sup>31,32</sup>



**Enzymatic Activity Studies.** Conjugation of a cationic tail longer than the oligonucleotide favors cell internalization and hybridization properties. We next evaluated if the natural oligonucleotide part of the conjugate is still recognized as a substrate for enzymes.

In particular, the cationic conjugate was tested as a primer for polymerase chain elongation. To ease detection and quantification, we chose to use the cationic conjugate as a primer for sequencing the pEGFP<sub>Luc</sub> plasmid by automatic means. 5 pmol of the oligonucleotide and 500 ng of the pEGFP<sub>Luc</sub> plasmid (the template) were added to the reaction mixture containing thermophile Taq polymerase, nucleotides triphosphates, and the fluorescently labeled nucleotide-triphosphate terminator in the appropriate buffer. The four reaction mixtures (one for each nucleobase) were then subjected to 25 cycles each consisting of plasmid denaturation (94 °C, 10 s), primer annealing (55 °C, 10 s), and elongation (60 °C, 3 min). After elimination of nucleotides by ethanol precipitation, the different fragments terminated at the 3' end with a fluorophore were separated by capillary electrophoresis. The plasmid sequencing with the 5'-unmodified CGA GGG CGA GGG CGA primer provided the expected histogram (Figure 8) and sharp separation of the different fragments. 5'-nd modification with hydrophobic tfa-protected (KKKR)<sub>5</sub>K or cationic (KKKR)<sub>5</sub>K peptide also allowed primer elongation, although capillary electrophoresis gave a degenerated fragment separation. Quantification of the fluorescence signal indicated that yields were about 10% and 30%, respectively (relative to the unmodified primer), indicating that the cationic domain perturbs only marginally the enzymatic recognition of the oligonucleotide 3'-end. Conversion of the histograms to nucleotide sequence and alignment with the original plasmid sequence provided good results with the unmodified and tfa-protected primers. However, alignment of the cationic tailed sequencing fragment was shifted by about 260 nt away from the priming site, certainly as a consequence of electrophoretic mobility perturbation of the short DNA fragments due to their cationic tail. Interestingly, despite nonoptimized separation, sequence alignment could be performed between the plasmid template and the DNA fragments originated from the cationic primer, suggesting that the cationic

conjugate annealed to the plasmid at the same site as the other ODNs. This indicates that 5'-cationic peptide-conjugated oligonucleotides remain substrates for DNA polymerase and that a cationic tail does not diminish Watson–Crick base pair recognition in a biological context.

## Conclusion

In summary, we have shown that cationic peptide–oligonucleotide diblock conjugates with a net positive charge can be synthesized. Charge reversal and aggregation properties enable cellular internalization into endosomes that can be ruptured by chloroquine, an endosomolytic compound. Moreover, the cationic tail allows stronger binding to the complementary nucleotide sequence. Finally, the cationic tail does not inhibit polymerase chain elongation. All together, these properties open novel perspectives for oligonucleotide applications without the use of delivery systems involving formulation of the nucleic acid. At this point, chloroquine is requested to rupture endosomal walls. Further improvement may be possible by modifying the peptide tail to include endosomolytic agents.<sup>33</sup> Moreover testing of these diblock conjugates in proven antisense<sup>34</sup> or silencing technologies<sup>35</sup> will require screening of a number of different oligonucleotide sequences for optimal inhibition and development of more versatile automatic synthesis.<sup>36, 37</sup>

**Acknowledgment.** We thank Isabelle Kuhn and Serge Vicaire for technical help in the sequencing reactions, Goudong Li and Pascale Buisine for acquiring MS data, and Edward Driggers for helpful discussions. This work was supported by grants from the Association Française contre les Myopathies and Vaincre la Mucoviscidose.

**Supporting Information Available:** Figures S1 and S2 are RP-HPLC traces showing that removal of tfa from a fluorescently tagged [tfa<sub>16</sub>-K(RKKK)<sub>5</sub>] peptide is achieved at 95% (1.5 h) and at 100% (5 h) after treatment with 28% NH<sub>4</sub>OH(aq). Figure S3 is supplementary characterization of protected conjugates by gel electrophoresis analysis. Figure S4 is a control showing that the longer unconjugated peptide does not modify the melting temperature of the DNA duplex in salt concentrations approaching physiological conditions. This material is available free of charge via the Internet at <http://pubs.acs.org>.

JA060873E

- (31) Demidov, V. V.; Protozanova, E.; Izvolsky, K. I.; Price, C.; Nielsen, P. E.; Frank-Kamenetskii, M. D. *Proc. Natl. Acad. Sci. U.S.A.* **2002**, *99*, 5953–8.
- (32) Kaihatsu, K.; Braasch, D. A.; Cansizoglu, A.; Corey, D. R. *Biochemistry* **2002**, *41*, 11118–25.
- (33) Pons, B.; Mouhoubi, L.; Adib, A.; Godzina, P.; Behr, J. P.; Zuber, G. *ChemBioChem* **2006**, *7*, 303–309.
- (34) Pan, W. H.; Clawson, G. A. *J. Cell Biochem.* **2006**, *98*, 14–35.
- (35) Hannon, G. J.; Rossi, J. J. *Nature* **2004**, *431*, 371–8.
- (36) Ocampo, S. M.; Albericio, F.; Fernandez, I.; Vilaseca, M.; Eritja, R. *Org. Lett.* **2005**, *7*, 4349–52.
- (37) Gait, M. J. *Cell Mol. Life Sci.* **2003**, *60*, 844–53.